A&A manuscript no.
(will be inserted by hand later)

Your thesaurus codes are:
03(11.05.2, 11.09.4, 11.14.1, 11.19.3)

ASTRONOMY
AND
ASTROPHYSICS
1.2.2008

A correlation between CO linewidth and starburst age in barred spiral galaxies ⋆

T. Contini[1], **H. Wozniak**[2], **S. Considère**[3], **and E. Davoust**[1]

[1] Observatoire Midi-Pyrénées, UMR 5572, 14 Avenue E. Belin, F-31400 Toulouse, France
[2] Observatoire de Marseille, URA CNRS 237, 2 Place Le Verrier, F-13248 Marseille Cedex 4, France
[3] Observatoire de Besançon, EP CNRS 123, B.P. 1615, F-25010 Besançon Cedex, France

Received 15 october 1996; accepted 12 december 1996

Abstract. New CO(1→0) and CO(2→1) profiles complemented by data from the literature are used to obtain CO linewidths for 29 barred spiral galaxies with young nuclear starbursts. The ages of the starbursts were estimated from optical spectroscopy and recent evolutionary synthesis models. The CO linewidths and the starburst ages are correlated : galaxies with young (4-6 Myr) starbursts display narrow ($\lesssim 100$ km.s^{-1}) CO line while those with older starbursts show broader CO lines. We discuss several scenarios of the gas dynamics during the nuclear starbursts' evolution to interpret the correlation.

Key words: Galaxies: evolution – Galaxies: ISM – Galaxies: nuclei – Galaxies: starburst

1. Introduction

Our understanding of the links between the gas dynamics and the star formation history in barred galaxies has made remarkable progress in the past ten years, thanks to numerous multi-wavelength observations and N-body simulations with stars, gas and star formation (Mihos & Hernquist 1994; Friedli & Benz 1995).

For instance, the suggestion of Shlosman et al. (1989) that the gas fuelling of the central regions is triggered by dissipation once the bar is formed has been confirmed and the efficiency of the process has been quantified (Friedli & Benz 1993). However, in order to accrete gas on a scale of a few parsec, another mechanism must be invoked, like a secondary bar or a triaxial bulge (Shlosman et al. 1989, 1990). These secondary bars have now been observed in the optical (Wozniak et al. 1995) and near infrared (Friedli et al. 1996) ranges, and in the CO line (Kenney 1996 and references therein). Friedli & Martinet (1993) have shown that double bar structures can transport amounts of gas much closer to the galactic center than simple bars. The gas accretion rate can be very high and may provide a possible mechanism for triggering starbursts.

However, it still remains to be shown that AGN or nuclear starbursts can be fuelled by such mechanisms. Indeed, high resolution observations (*Hubble Space Telescope* images, CO mappings) are beginning to reveal complex structures that simulations cannot accurately model because of their poor resolution in the innermost region.

In order to shed new light on the relationship between nuclear starbursts and gas dynamics, we decided to combine the properties of molecular clouds with characteristics of the starbursts rarely used in previous studies. In particular, the age of the starburst has so far never been used in practice; it can be now estimated from optical spectroscopy and evolutionary synthesis models.

2. Observations and data analysis

2.1. Sample selection and properties

We selected 29 galaxies (cf. Table 1) from a large sample of starburst galaxies (Contini 1996). They share the following properties: 1) they host a young nuclear starburst (age ranging from 3 to 12 Myr) and 2) they have the largest far infrared fluxes. The latter criterion was to optimize our chances of detecting CO.

All galaxies of the sample are barred galaxies. This classification comes from the LEDA database and/or from our CCD images at a resolution of 1.5″ (Contini 1996). Most galaxies have morphological peculiarities, either an asymmetric spiral pattern (Mrk 133, 213, 353, 691, 799, 1466 and, to a lesser extent, Mrk 759 and 1050), several bright HII regions along the bar (Mrk 13, 281, 306, 710, 712, 731, 1341), or a polar ring (Mrk 306). Some

Send offprint requests to: wozniak@observatoire.cnrs-mrs.fr

⋆ Based on observations obtained at the 30 meter radiotelescope on Pico Veleta, operated by IRAM and the 1.93 meter telescope of Observatoire de Haute-Provence, operated by INSU (CNRS).

galaxies also have a close companion (Mrk 306, 602, 691, 1379). Mrk 2 has a companion 103″ away and Mrk 617 is a merger. The only galaxies without marked peculiarities are Mrk 52, 412, 545, 575, 708, 1088, 1194 and 1485. Two galaxies lacked high resolution images (Mrk 1365 and 1379).

2.2. CO line profiles

The radio observations were obtained at the IRAM 30 meter radiotelescope on August 20 to 24, 1995. We observed in single sideband at two frequencies simultaneously, CO(1→0) at 115.3 Ghz with the 1.3mm SIS receiver, and CO(2→1) at 230.5 Ghz with the 3mm (230G1) SIS receiver. The beamwidth of the 30 meter antenna is 21″ and 12″, and the main beam efficiency 0.75 and 0.39 at 115 and 230 Ghz respectively. The observing procedure and data reduction are detailed in Contini (1996).

We observed 18 galaxies of the sample; CO data for the other 11 galaxies were taken from the literature. Mrk 712 is the only undetected galaxy at 115 Ghz; this is not surprizing, as its far infrared flux turns out to be the lowest of the whole sample. Mrk 412, which also has a low far infrared flux, was barely detected at 115 GHz. Several galaxies, Mrk 13, 759, 1050, 1341, were ambiguously detected at 230 Ghz, mainly because the noise at that frequency was a factor 2 or 3 higher than at 115 GHz. Mrk 213 was probably detected at 230 Ghz, but the adopted recession velocity was too low, and, consequently, part of the profile was outside the observing frequency window.

The CO(1→0) and CO(2→1) line profiles are displayed in Contini (1996). The spectra were smoothed to a final velocity resolution of 10 km s^{-1} for both transitions. One of the main characteristics of the profiles is that they are generally not symmetric ; this cannot be attributed to noise, because of the long integration times (typically between 50 and 330 minutes) and the good resulting signal-to-noise ratio. Most profiles can be adjusted by two or three gaussians; this suggests the existence of separate molecular clouds of uneven sizes and/or with distinct velocities. Only six profiles (those of Mrk 13, 133, 412, 1050, 1379 and 1485) are well fitted by one gaussian.

The CO linewidths were measured directly on the profiles rather than by a multi-gaussian fit, because, when several components are present in the profile, the gaussians overlap and the FWHM thus does not reflect the width of the profile. The linewidths were determined both at 20 and 50% of the maximum intensity for our sample as well as for the data taken from the literature. We used these two estimates of the linewidths to check the consistency of our results. For the galaxies with high signal-to-noise ratio, the uncertainty on the linewidth is equal to the velocity resolution (10 km s^{-1}). The linewidths of CO(1→0) and CO(2→1) profiles at 20 and 50% are given in Table 1. As the observing conditions (e.g. the beamsize) and the calibration procedures for the 11 galaxies from the literature were in general different from ours, these data are rather heterogeneous and have been used with caution; they are thus listed separately in Table 1 and plotted with different symbols in Fig. 1.

Table 1. CO linewidths and starburst ages of the sample of barred Markarian galaxies. W(CO) is the width of the line estimated at 20 and 50% of the maximum intensity of the CO profiles. Multiple entries correspond to different HII regions with comparable Hβ fluxes

Mrk	W(CO) 50%		W(CO) 20%		age		Ref.
	(1→0)	(2→1)	(1→0)	(2→1)	CMH94	LH95	
	(km s^{-1})		(km s^{-1})		(Myr)		
2	106	84	133	130	5.6	8.6	
13	78		122		5.3	4.8	
133	83	78	94	116	4.5	8.1	
213	311		389		7.5	7.2	
306	67	49	161	95	7.4	7.0	
353	278	259	306	330	8.0	9.0	
412	78		111		5.6	4.9	
575	117	108	150	149	7.0	8.5	
602	194	189	278	254	5.7	8.8	
691	100	59	144	138	5.4	4.9	
712							
731	100	57	128	73	4.4	7.9	
759	167		172		9.0	11.0	
1050	250		328		8.0	9.0	
1341	155		200		5.7	8.7	
1365	217	181	267	249	9.8	9.4	
1379	72	59	111	95	3.9	4.5	
					5.4	4.9	
					5.7	8.6	
1485	240	278	361	414	11.2	10.0	
52	60		133		4.0	6.3	2
281	278		300		6.5	7.5	1
534	420		482		8.0	8.9	3
545	364	348	473	435	6.0	9.2	5
617	255	287	327	348	7.4	8.5	5
708	187	188	275	291	5.7	8.8	4
710		73		137	4.0	6.3	6
					4.8	7.7	6
					5.5	8.4	6
799	309	322	400	400	6.0	9.2	5,6
1088	400	157	509	365	8.5	9.2	5
1194	291	130	364	226	9.0	11.0	5
1466	127	127	182	174	5.3	8.2	5

References to CO linewidths (last col., bottom half of the Table):
1 = Jackson et al. (1989); 2 = Young et al. (1995);
3 = Wiklind & Henkel (1989); 4 = Chini et al. (1992);
5 = Krügel et al. (1990); 6 = Contini et al. (1996).

2.3. Optical spectra and starburst ages

The CCD spectra were obtained during several runs at the 1.93 meter telescope of Observatoire de Haute-Provence, with the Carelec spectrograph. We took long-slit spectra at 260Å/mm. We observed standard stars for flux calibration. The spectra were reduced with MIDAS. The deblending of the Hα+[NII] and [SII]$\lambda\lambda$6716,6731 lines was done by fitting multigaussian profiles, with constraints on the relative positions of the individual lines.

The starburst ages were estimated from the equivalent widths W(Hβ) and metallicities (estimated from the oxygen abundance) measured on our spectra and the evolutionary synthesis models of Cerviño & Mas-Hesse (1994, CMH94) and Leitherer & Heckman (1995, LH95). We used

a standard Salpeter Initial Mass Function (IMF) with $\alpha = 2.35$, $M_{\rm inf} = 1$ to 2 $M_\odot$ and $M_{\rm sup} = 100$ to 200 $M_\odot$. W(Hβ) was corrected for Balmer absorption (assuming $W^{\rm abs}(H\beta) \simeq 2$ Å) which is a contamination from the underlying stellar population. The procedure for estimating the starburst ages is fully described in Contini et al. (1995) and Contini (1996). When several HII regions (or even a fraction of a giant HII region) fall inside the beam of the radiotelescope, the age is that of the brightest region in Hα. HII regions outside the beam were not taken into account. Incidentally, the brightest HII regions are all nuclear, except for Mrk 13 (4.3″ from the center) and Mrk 306 (7.8″ from the center).

Three HII regions of Mrk 306 have similar (within a factor 2) Hα luminosities. But the various ages are comparable for both models (7.3 to 7.4 Myr using CMH94 and 7.0 to 8.5 Myr using LH95), so that we adopted a mean value for the age. The three HII regions of Mrk 710 also have similar Hα luminosities, but the ages range from 4 to 5.5 Myr (CMH94) and 6.3 to 8.4 Myr (LH95). We thus kept three entries in our data for this object. For Mrk 1379, two HII regions lie near the nucleus with very different ages (3.9, 5.7 using CMH94; 4.5, 8.6 using LH95). Although the ratio of Hα luminosities is close to 9, we decided to keep both regions in our subsequent analysis.

A conservative estimate of the error on the age of young starbursts is 1 Myr for both models, taking into account the possible uncertainties on the slope of the IMF, the contamination by older or younger HII regions on the borderline of the beam, etc. For older starbursts, Hβ is weaker and the uncertainty on the age increases, and reaches 2 Myr for 10 Myr old bursts. However, there are several galaxies for which the ages differ between CMH94 and LH95 models by more than the sum of the age errors. *We thus decided to keep only the objects showing a difference in age less than 2.5 Myr.* The final age is thus the mean of the two estimates. This criterion does not reduce the number of young starbursts displayed in Fig. 1 with respect to those listed in Table 1. But fewer old starbursts are displayed, since there the error on the age difference may reach ∼4 Myr.

3. The CO linewidth – starburst age correlation

The CO linewidth as a function of starburst age is plotted in Fig. 1 with the data of Table 1. When the two linewidths are comparable, we only plot the one at 115 GHz, for the sake of clarity. To correct for projection effects onto the plane of the sky, we divided the observed width by $2\sin(i)$, where i is the inclination of the galaxy taken from the LEDA database. For the top diagram we used the *mean* of the two starburst ages determined in the previous section. We also show separate diagrams for the CMH94 and LH95 models, since they often give significantly different age estimates.

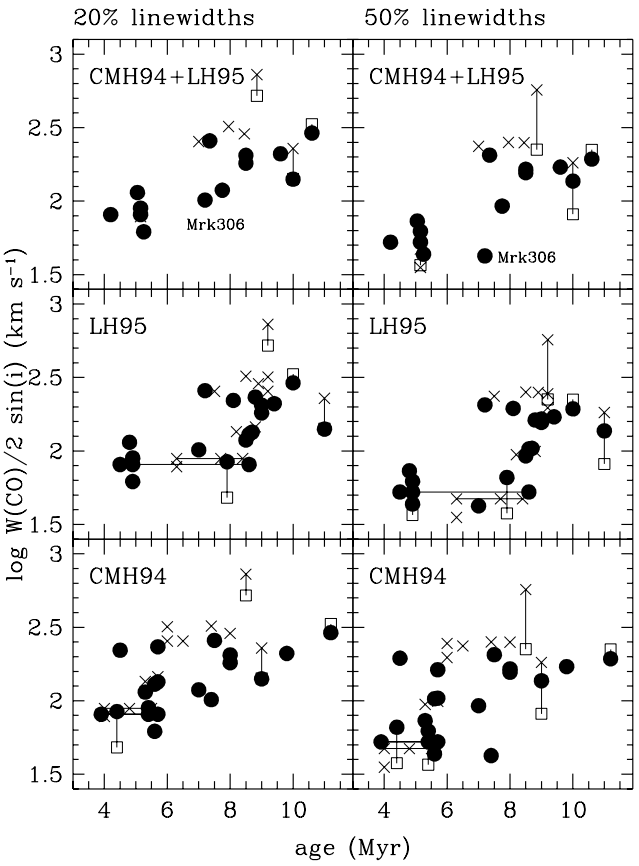

Fig. 1. CO linewidth versus starburst age estimated from the models of LH95 (*middle* panel) and CMH94 (*bottom* panel). The *top* panel is for the mean of the ages predicted by the two models. •: CO(1→0) for our sample; ×: CO(1→0) for data from literature; □: CO(2→1), when it is different from CO(1→0). Different data for the same object are joined by a line. Linewidths are measured at 20% (*left* panels) and 50% (*right* panels) of the maximum intensity of the CO profile

A correlation appears in the diagrams using the mean and LH95 ages. Narrow CO linewidths (less than 100 km s^{-1}) are associated with young starbursts while older starbursts show greater linewidths (between 150 and 300 km s^{-1}). There is one apparent exception, Mrk 306, which has an older starburst and a narrow linewidth, but the CO line profile shows several components, only one of which is taken into account in the measure of the linewidth, because it is at least twice as strong as the two others.

We have checked that the correlation between CO linewidth and starburst age does not depend on the distance or on the absolute magnitude (or, equivalently, the mass) of the galaxy; narrow linewidths are not associated with low mass objects. We have also verified that the CO linewidth is *independent* of the HI linewidth.

The dispersion in Fig. 1 may have several causes. The dispersion in starburst ages could be due to the contami-

nation by younger extra-nuclear HII regions. It could also partly be due to errors on the ages, which range from 1 to 2 Myr. The dispersion in the CO linewidths could be attributed to external causes like the interaction with a companion. Let us recall that most galaxies of our sample are peculiar in one way or another (cf. Sect. 2.1). It could also be partly due to the uncertainties on the angle i.

There could also be internal causes, such as the resolving power of the radiotelescope at different frequencies. When the CO linewidth at 115 and at 230 Ghz are different, this may mean that the CO emission is resolved at the lower frequency. But different linewidth at the two frequencies may also be due to different physical conditions; this seems to be the case for Mrk 1485, for which the linewidth at the higher frequency is larger than that at the lower frequency.

Furthermore, in Mrk 306, there is a great difference between the CO(1→0) and CO(2→1) linewidths. The difference is due to the position of the most luminous HII region which is 7.8″ from the nucleus, inside the CO(1→0) beam but outside the CO(2→1) one; for this galaxy, we only retained the CO(1→0) data.

4. Discussion

Let us now interpret the correlation between CO linewidth and starburst age. We restrict the discussion to the evolution of starbursts and CO distributions in the central regions of galaxies, since the starburst ages of our sample are those of *nuclear* HII regions.

The first explanation that comes to mind is that the molecular clouds are initially concentrated right near the nucleus ($r \leq 100$ pc). The lines are broadened by galactic rotation, assuming a standard rotation curve (Sofue 1996) and/or by the velocity dispersion among individual clouds due to the kinetical energy from supernovae and stellar winds associated with the starburst (Irwin & Sofue 1996). As the starburst ages, the gas expands outward ($r \sim 500$ pc) and the lines become wider because the clouds take part in the galactic rotation. The problems with this scenario are that most of the gas must stay in the disk and that there is no physical mechanism by which the clouds can acquire enough angular momentum to participate to the galactic rotation. This is moreover in contradiction with the fact that the gas on the contrary tends to lose angular momentum (in the inflow scenario).

A classical gas inflow cannot explain the correlation either, since it predicts that the starbursts may be ignited in a circum-nuclear ring before the gas reaches the center, and young starbursts with broad CO lines are expected.

Another possibility is that the clouds are pushed outward, preferentially out of the plane of the galaxy, by powerful outflowing winds generated by supernova explosions (Heckman et al. 1990). The broadening of the lines is then due to expansion rather than to rotation. The problem here is that the line profiles should be double peaked, which is generally not the case in our sample.

Finally, the correlation could be spurious, if galaxies with young starbursts are nearly face-on or have a low mass, but this is not the case here.

None of the above scenarii, outflow of molecular gas inside or out of the disk, are completely satisfactory. This correlation remains a puzzling problem which deserves more work. On one hand, the numerical simulations must increase both their spatial and temporal resolutions and include an energetic starburst in the nucleus of galaxies. On the other hand, we must acquire higher resolution ($\lesssim$ 100 pc) CO observations in the nuclei of galaxies at different stages of starburst evolution.

Acknowledgements. Data from the literature were obtained with the Lyon Meudon Extragalactic database (LEDA), supplied by the LEDA team at CRAL-Observatoire de Lyon (France). We thank Raphaël Moreno (IRAM) and the staff of OHP for assistance at the telescopes. We thank the referee, I. Shlosman, for fruitful comments.

References

Cerviño M., Mas-Hesse J.M., 1994, A&A 284, 749
Chini R., Krügel E., Steppe H., 1992, A&A 255, 87
Contini T., 1996, PhD thesis, Université Paul Sabatier, Toulouse, France
Contini T., Davoust E., Considère S., 1995, A&A 303, 440
Contini T., Wozniak H., Considère S., Davoust E., 1996, A&A, submitted
Friedli D., Benz W., 1993, A&A 268, 65
Friedli D., Benz W., 1995, A&A 301, 649
Friedli D., Martinet L., 1993 A&A 277, 27
Friedli D., Wozniak H., Rieke M., Bratschi P., Martinet L., 1996, A&AS 118, 461
Heckman T.M., Armus L., Milet G.K., 1990, ApJS 74, 733
Irwin J.A., Sofue Y., 1996, ApJ 464, 738
Jackson J.M., Snell R.L., Ho P.T.P., Barrett A.H., 1989, ApJ 337, 680
Kenney J.D.P., Carlstrom J.E., Young J., 1993, ApJ 418, 687
Kenney J.D.P., 1996, in Barred Galaxies, IAU Coll. 157, R.Buta, D.A. Crocker, B.G.Elmegreen (Eds.), 150
Krügel E., Steppe H., Chini R., 1990, A&A 229, 17
Leitherer C., Heckman T.M., 1995, ApJS 96, 9
Mihos J.C., Hernquist L.E., 1994, ApJ 425, L13
Shlosman I., Frank J., Begelman M.C., 1989, Nature, 338, 45
Shlosman I., Begelmann M.C., Frank J., 1990, Nature 345, 679
Sofue Y., 1996, PASJ in press
Young J.S., Xie S., Tacconi L., et al., 1995, ApJS 98, 219
Wiklind T., Henkel C., 1989, A&A 225, 1
Wozniak H., Friedli D., Martinet L., Martin P., Bratschi P., 1995, A&AS 111, 115

This article was processed by the author using Springer-Verlag LaTeX A&A style file *L-AA* version 3.